Kinetics of p-Xylene Liquid-Phase Catalytic Oxidation to Terephthalic Acid

ARTICLE *in* INDUSTRIAL & ENGINEERING CHEMISTRY RESEARCH · DECEMBER 2004

Impact Factor: 2.59 · DOI: 10.1021/ie049372x

5 AUTHORS, INCLUDING:

Youwei Cheng
Zhejiang University
63 PUBLICATIONS **401** CITATIONS

SEE PROFILE

KINETICS, CATALYSIS, AND REACTION ENGINEERING

Kinetics of *p*-Xylene Liquid-Phase Catalytic Oxidation to Terephthalic Acid

Qinbo Wang,* Xi Li, Lijun Wang, Youwei Cheng, and Gang Xie

Department of Chemical Engineering, Zhejiang University, Hangzhou, 310027 Zhejiang, People's Republic of China

A fractional kinetic model for the liquid-phase oxidation of *p*-xylene to terephthalic acid catalyzed by cobalt acetate and manganese acetate and promoted by hydrogen bromide was proposed. The developed model parameters were determined in a nonlinear optimization, minimizing the difference between the simulated and experimental time evolution of the product composition obtained in a semibatch oxidation reactor where the gas and liquid phases were well mixed. The experiments included four values of the initial concentration of *p*-xylene. Further, the effects of the oxygen partial pressure, reaction temperature, catalyst concentration, and promoter concentration on the time evolution of the experimental product distribution and kinetic constants of the developed model were investigated.

Introduction

As one of the most important aromatic compounds, terephthalic acid (TA) is widely used in organic synthesis, particularly in the polyester industry. Commercially, the majority of TA is produced by the air oxidation of *p*-xylene (PX) in acetic acid (HAc) in the temperature range from 180 to 205 °C, catalyzed by cobalt acetate ($Co(Ac)_2$) and manganese acetate ($Mn(Ac)_2$) and promoted by hydrogen bromide (HBr).[1] To gain better insight into the reaction mechanism and identify the effects of different parameters on the progress of the reaction, it is essential to study the kinetics. Further, the rational design, optimization, control, and analysis of the oxidation of PX to TA process also require knowledge of the kinetics.

The oxidation of PX to TA occurs through radical chain elementary reactions, which involve a very large number of radicals as well as molecular species. Emanuel proposed a detailed radical chain mechanism of the liquid-phase cobalt catalyzed oxidation of PX.[2] However, the complexity of this reacting system clearly prevents the evaluation of the individual values of the kinetic constant by direct fitting of the model results against the experimental data, mostly because of the inability of measuring the concentration of the radical species. The most common approach is to lump the detailed mechanism into a set of global reactions which involve only molecular species, whose concentration can be, in principle, easily monitored as a function of time.[3] Without involving a formal procedure of general validity but simply including the minimum number of reactions to describe the behavior of all the species of interest, various lumped kinetic schemes for the homolytic oxidation process have been developed in the literature for PX oxidation. By accounting for the most important intermediates and final products of the process, that is, *p*-tolualdehyde (TALD), *p*-toluic acid (PT), 4-carboxybenzaldehyde (4-CBA), and TA, Yan has recently proposed the lumped kinetic model as shown in Figure 1 for the liquid-phase oxidation of PX to TA,[4] where the reactions of PX to TALD and PT to 4-CBA involve the addition of $1O_2$ and the reactions of TALD to PT and 4-CBA to TA involve the addition of $^1/_2O_2$. Cao and Cincotti studied the kinetic scheme at low temperature and assumed that all the reactions were zeroth order with respect to gaseous reactants under the condition that the oxygen partial pressure was higher than a minimum value and first order with respect to liquid reactants.[5−8] Yan studied the oxidation kinetics at high temperature and also assumed that all the reactions were 0.65th order with respect to PX and first order with respect to the other liquid reactants, and the effect of oxygen partial pressure on the reaction rate was neglected.[4] However, when the *n*th reaction kinetics was used in an industrial oxidation process, there was a significant difference between the simulated results and the industrial operating results. It was mainly because the kinetics previously obtained was empirical and did not reveal the reaction mechanism sufficiently. Recently, Wang developed the kinetic model as shown in eq 1 from the radical chain reaction mechanisms.[9]

$$r_j = k_j \frac{C_j}{(\sum_{i=1}^{4} d_i C_i + \theta)^{\beta_j}} \qquad j = 1-4 \qquad (1)$$

When eq 1 was used to describe the effect of the reaction factors on the reactions in the industrial reactor, the predicted oxidation results agreed with the industrial results satisfactorily.[10] In this work, the experiments to determine the kinetic model constants of eq 1 were reported. The experiments included four values of the initial concentration of *p*-xylene. Further, the effects of the oxygen partial pressure, reaction temperature, catalyst concentration, and promoter con-

10.1021/ie049372x CCC: $30.25
Published on Web 12/23/2004

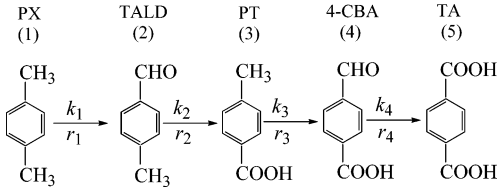

Figure 1. Lumped kinetic scheme for the oxidation of *p*-xylene to terephthalic acid.

Table 1. Operating Conditions for the Experimental Runs

run	T (°C)	$C_{PX,0}$ (mol/ kg_{HAc})	P_{O_2} (kPa)	C_{Co} (10^4 kg/ kg_{HAc})	C_{Mn} (10^4 kg/ kg_{HAc})	C_{Br} (10^4 kg/ kg_{HAc})
1	191	3.145	40.0	350	326	475
2	191	1.887	40.0	350	326	475
3	191	0.943	40.0	350	326	475
4	191	0.472	40.0	350	326	475
5	191	0.943	12.0	350	326	475
6	191	0.943	20.0	350	326	475
7	191	0.943	28.0	350	326	475
8	185	0.943	40.0	350	326	475
9	188	0.943	40.0	350	326	475
10	194	0.943	40.0	350	326	475
11	197	0.943	40.0	350	326	475
12	191	0.943	40.0	250	233	339
13	191	0.943	40.0	450	419	610
14	191	0.943	40.0	550	512	746
15	191	0.943	40.0	350	326	237
16	191	0.943	40.0	350	326	712
17	191	0.943	40.0	350	326	949

centration on the time evolution of the experimental product distribution and kinetic constants of the developed model were investigated.

Experimental Setup and Procedure

The experimental apparatus, sampling apparatus, and analytical methods used in this work were described elsewhere.[11] Briefly, it consisted of a 500 mL titanium reactor maintained at the desired temperature through forced circulation of diathermic oil and wall electric heating. Both the liquid and gaseous phases were continuously stirred. The system was equipped with three condensers in order to ensure complete condensation and recycling of the evaporated compounds. The reactor temperature was continuously monitored during the experimental runs with a thermal resistance thermometer. In a typical experimental run, the reactor was charged with 300 mL mixtures of proposed PX, HAc, and catalyst. After the temperature reached the desired value, the gas (air) was then continuously fed through the liquid. The experimental runs were carried out under the conditions summarized in Table 1. The reproducibility of the experimental runs was verified by repeating each of them at least twice. The experimental runs reported in Table 1 were performed at 900 rpm, since the influence of stirring speed of this value on the product distribution was found to be negligible. A special sampler was used to sample the reaction products. The low boiling temperature components such as PX, HAC, and TALD were analyzed by gas chromatography (GC) (Shimadzu GC-9A), and the high boiling temperature components such as PT, 4-CBA, and TA were analyzed by high pressure liquid chromatography (HPLC) (Shimadzu-6A). Isopropyl benzene was used as the internal standard substance to correlate the data obtained from GC and HPLC analyses.

Semibatch Reactor Model

By taking into account only the formation of the molecular species that represented the most important intermediate and final product, the lumped kinetic scheme as shown in Figure 1 and the kinetic model of eq 1 was used. The description of the diffusion and reaction processes at the gas−liquid interface was neglected because of the elimination of mass transfer influence. Since all experiments were performed under the kinetic regime, the following mass balances were used:

$$\frac{dC_j}{dt} = \sum_{i=1}^{4} \nu_{i,j} r_j \qquad j = 1-4 \tag{2}$$

along with the initial conditions

$$C_j = C_{j,0} \qquad j = 1-4 \tag{3}$$

The energy balance was not considered here, since the reactor had been operated under isothermal conditions.

The kinetic parameters were determined in a nonlinear optimization, minimizing the difference between the simulated and the experimental time evolution of the product composition of experimental runs 1−4. The fourth-order Runge−Kutta method was used to solve eq 2, and the simplex method was used in the nonlinear optimizations. The method is implemented in the Matlab Optimization Toolbox (The Mathworks). The simulation was written in Matlab to use their optimization routine.

Results and Discussion

Kinetic Parameter Evaluation. The time evolution of the experimental product composition along with the simulated value for experimental runs 1−4 is summarized in Figure 2. A comparison between the simulated results and the experimental data is also shown in Figure 2, where it can be seen that the obtained agreement is in general satisfactory. The average relative deviation of the simulated value and the experimental data is <5%. This model is able to predict the reactor behavior as a function of the concentration of the liquid reactants. The obtained kinetic parameters are given in Table 2.

Effect of Oxygen Partial Pressure. In the literature, when the PX oxidation process was studied, the oxygen partial pressure was kept at a high value so that the effect of the oxygen partial pressure on the oxidation process could be neglected. Cao and Cincotti studied the PX oxidation process with air and pure oxygen catalyzed by the cobalt naphthenate in a semibatch reactor,[5−8] but the studies were carried out at a low temperature of 80−130 °C and atmospheric pressure. They assumed the PX oxidation process was zeroth order with respect to the oxygen partial pressure. Digruov found that the oxidation of PX was independent of the oxygen partial pressure at a temperature of 70−105 °C and an oxygen partial pressure of 20−100 kPa.[12] Unfortunately, in the industrial reactors, the volume fraction of oxygen in the offgas is controlled within 4−5% for safety[10] and the corresponding oxygen partial pressure is 10−20 kPa. At such a low oxygen partial pressure, the reaction is no longer zeroth order with respect to the oxygen partial pressure. To obtain a kinetic model which can be used in industrial processing, experiments of different oxygen

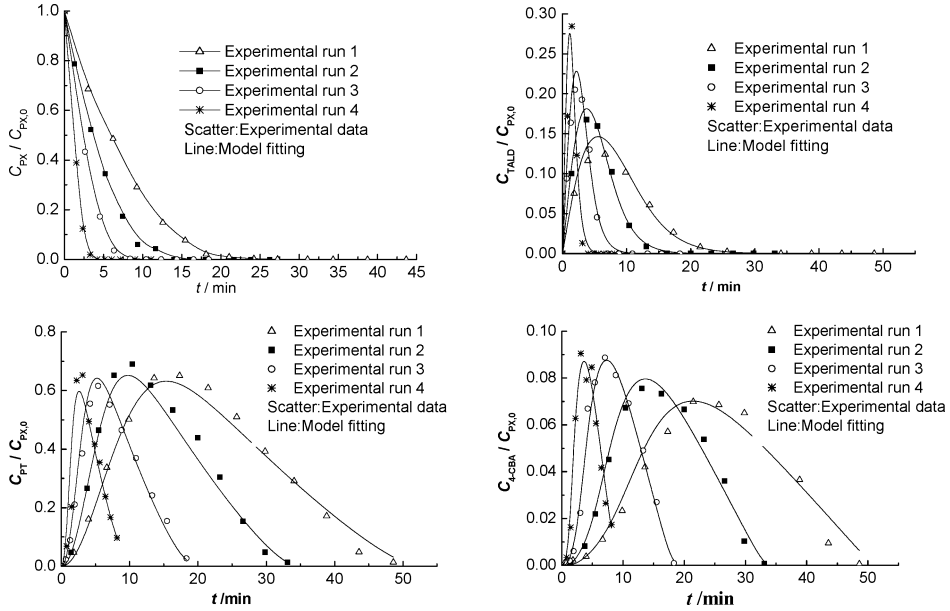

Figure 2. Evolution of the experimental and simulated product composition for experimental runs 1−4. The parameters in the simulation are from the optimization, Table 2.

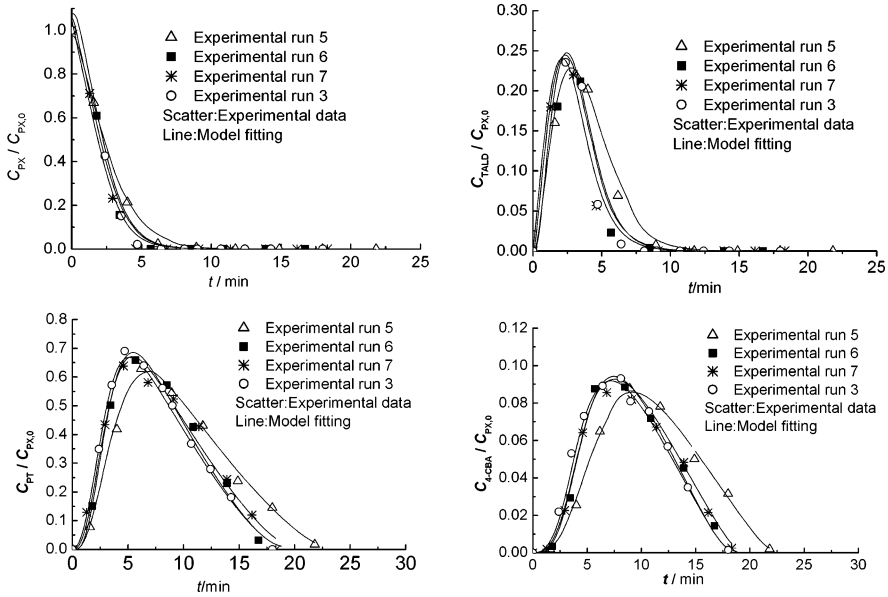

Figure 3. Evolution of the experimental and simulated product composition for experimental runs 3 and 5−7. The parameters in the simulation are from the optimization.

Table 2. Optimal Parameters from Optimizations with Experimental Runs 1−4

	k_i (min^{-1})	d_i (kg$_{HAc}$/mol)	β	θ
$i = 1$	0.1716	1.4247	0	0.0146
$i = 2$	0.7002	0	0.5254	
$i = 3$	0.0353	0	0	
$i = 4$	0.3296	4.8419	0.8111	

partial pressures were performed. The experimental conditions are listed in Table 1. The experimental results obtained from experimental runs 3 and 5−7 are illustrated in Figure 3, and the rate constants are given in Table 3. The results show that the effect of the oxygen partial pressure on the reactions decreases with the increase of partial pressure over a threshold value of 28.0 kPa. In the range 10−20 kPa of industrial reaction conditions, the oxygen partial pressure influences the reaction significantly. That is one of the reasons that when the kinetic model of Yan was used to model the industrial reactor, correction coefficients must be introduced into the rate constants.

Table 3. Optimal Reaction Rate Constants for Experimental Runs 3 and 5−17

run	k_1 (min^{-1})	k_2 (min^{-1})	k_3 (min^{-1})	k_4 (min^{-1})
3	0.176	0.725	0.0361	0.338
5	0.138	0.547	0.0276	0.257
6	0.162	0.656	0.0329	0.307
7	0.176	0.723	0.0366	0.339
8	0.139	0.590	0.0256	0.248
9	0.153	0.650	0.0303	0.288
10	0.189	0.762	0.0409	0.386
11	0.216	0.863	0.0479	0.436
12	0.119	0.513	0.0250	0.253
13	0.211	0.841	0.0472	0.433
14	0.217	0.908	0.0568	0.521
15	0.099	0.507	0.0232	0.220
16	0.205	0.837	0.0473	0.461
17	0.219	0.855	0.0578	0.531

Effect of Temperature. PX liquid-phase oxidation at 185, 188, 191, 194, and 197 °C was carried out to

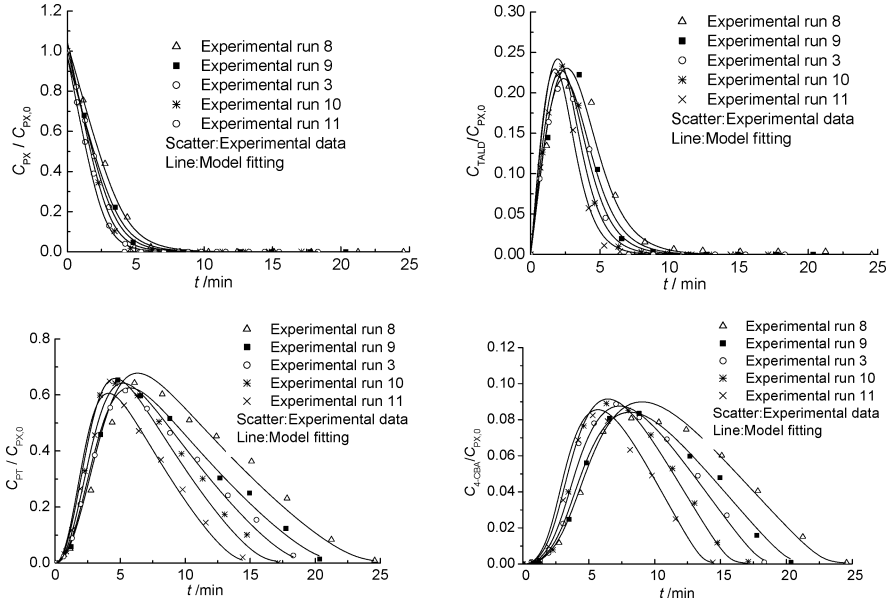

Figure 4. Evolution of the experimental and simulated product composition for experimental runs 3 and 8−11. The parameters in the simulation are from the optimization.

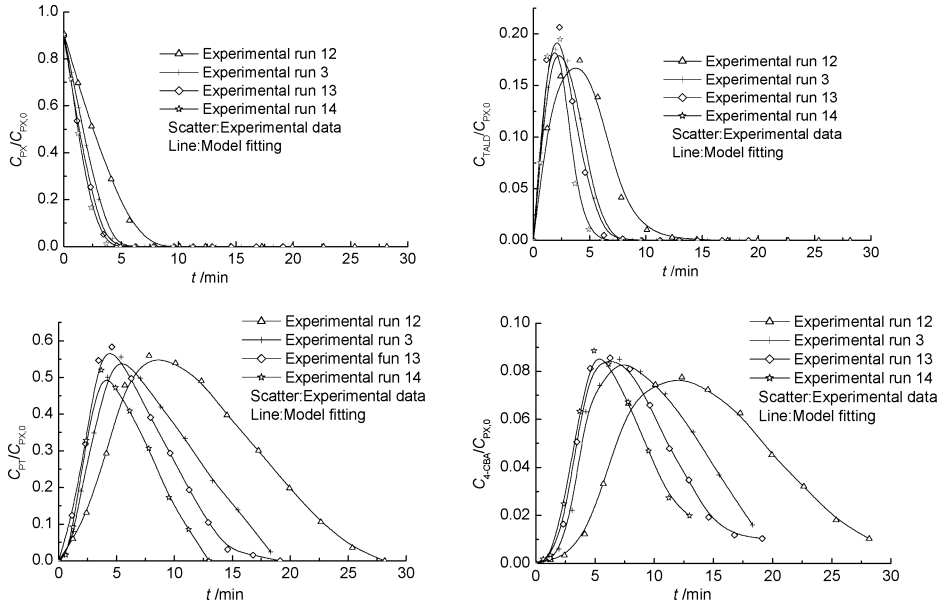

Figure 5. Evolution of the experimental and simulated product composition for experimental runs 3 and 12−14. The parameters in the simulation are from the optimization.

Table 4. Optimized Kinetic Constants and Activity Energy

k_i	$i = 1$	$i = 2$	$i = 3$	$i = 4$
E_i (kJ/mol)	65.5	54.9	92.8	84.9
$k_{i,0}$ (min^{-1})	4.07×10^6	1.08×10^6	9.80×10^8	1.17×10^9
variance (R^2)	0.998	0.995	0.999	0.997

investigate the temperature effect. Plots of $C_j/C_{PX,0}$ as a function of time for experimental runs 3 and 8−11 are shown in Figure 4.The kinetic model of eq 1 is employed to fit the data. A comparison between the simulated results and the experimental data is also shown in Figure 4. The optimal rate constants at each temperature are shown in Table 3. From Figure 4 and Table 3, it can be seen that the reaction temperature has a strong effect on the reaction rate of each step and the reaction rate was found to increase with an increase in the reaction temperature. The rate constants obtained can be well represented by the Arrhenius relationship and the optimized kinetic constants and activity energy for each oxidation step are shown in Table 4. The obtained activation energy of different reaction steps ranges from 54.9 to 92.8 kJ/mol; among them, the activation energy of the PT to 4-CBA step is the highest (92.8 kJ/mol) and that of the 4-CBA to TA step is the second highest (84.9 kJ/mol); these are remarkably higher than the values of the other steps (54.9−65.5 kJ/mol). This fact shows that oxidation of the second methyl group of PX is more sensitive to the temperature variation than the first one.

Effect of Catalyst Concentration. Plots of the quantity $C_j/C_{PX,0}$ as a function of time for each component at various catalyst concentrations are shown in Figure 5, while fixing the mass ratio of $[Co^{2+}]/[Mn^{2+}]/[Br^-]$ at 1. The values of the kinetic constants appearing in the lumped kinetic scheme shown in Figure 1 are then estimated by fitting the time evolution of the experimental product composition of runs 3 and 12−14 in Table 1 through an optimization procedure using the

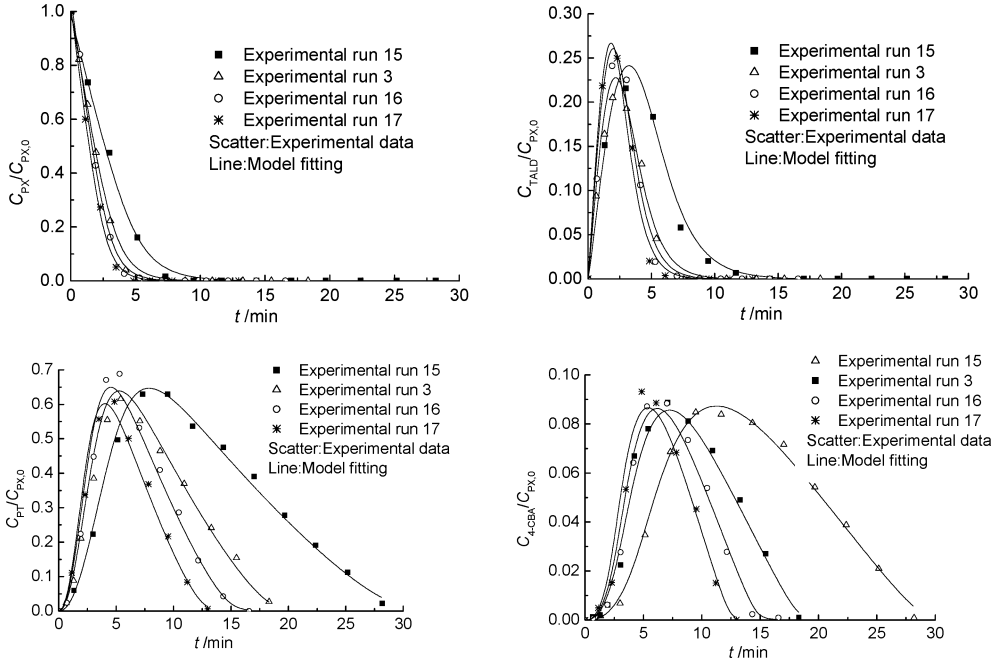

Figure 6. Evolution of the experimental and simulated product composition for experimental runs 3 and 15−17. The parameters in the simulation are from the optimization.

model given by eqs 1−3, and they are shown in Table 3. A comparison between the model results and the experimental data is also shown in Figure 5, where it also may be seen that the obtained agreement is generally satisfactory. This allows us to confirm that the lumped kinetic scheme retains a level of process description detailed enough to characterize the distribution of the most important products when changing catalyst concentration within a relatively wide range. From Table 3, we can conclude that the reaction rates are much more concentration-sensitive at a low catalyst concentration than at a high catalyst concentration. It is seen that the rate constants k_1 and k_2 increase eventually with the increasing catalyst concentration, reaching a plateau, but the rate constants k_3 and k_4 increase almost linearly with the increasing catalyst concentration.

Effect of Promoter. If the catalyst system only including [Co^{2+}] and [Mn^{2+}] is used in the catalytic oxidation of PX, not only the oxidation rate but also the yield of TA will be very low. A promoter must be introduced into the catalytic system.[13] HBr is a common promoter widely used in the industrial oxidation of PX to TA. It is necessary to study the effect of [Br^-] on the oxidation rate. Plots of the quantity $C_j/C_{PX,0}$ as a function of time for experimental runs 3 and 15−17 in Table 1 are shown in Figure 6. The optimal values of the kinetic constants are shown in Table 3. A comparison between the simulated results and the experimental data is also shown in Figure 6, where it also may be seen that the obtained agreement is generally satisfactory.

A concentration effect the same as the catalyst concentration effect on the oxidation rate is found for [Br^-]. The reaction rates of PX to TALD and TALD to PT increase by 25%; also the reaction rates of PT to 4-CBA and 4-CBA to TA increase by more than 60% when [Br^-]/[Co^{2+}] increases from 1 to 2, which clearly shows that [Br^-] accelerates the reaction rate significantly. The higher [Br^-] is, the faster the reaction will be. However, considering the discharge of the pollutants and the corrosion of the equipment, it is not a wise choice to run the oxidation process at a high level of [Br^-]. In industries, the selected [Br^-]/[Co^{2+}] ratio is $\sim 1/2-1$.

Conclusions

Some kinetic aspects of the air oxidation of PX in HAc in the temperature range from 184 to 197 °C, catalyzed by $Co(Ac)_2$ and $Mn(Ac)_2$ and promoted by HBr, are examined in this work from the experimental point of view. The effect of various operating variables, that is, temperature, oxygen partial pressure, initial PX concentration, catalyst concentration, and promoter concentration, is analyzed. A model for the description of the semibatch gas−liquid reactor for PX oxidation has been developed. The proposed reactor model is based on a lumping kinetic scheme and a fractional-like kinetic model of the complex radical chain mechanism of the oxidation process, where only the most important compounds detected experimentally, that is, TALD, PT, 4-CBA, and TA, are taken into account. The model parameters and rate constants are determined in a nonlinear optimization, minimizing the difference between the simulated and experimental time evolution of the product composition. A comparison between model prediction and experimental data is also presented, and the agreement is quite satisfactory. The obtained results confirm the fractional kinetic model.

Acknowledgment

The financial support by the National Science Foundation of China (no. 20076039) and SINOPEC (no. X500029) is gratefully acknowledged.

Notation

C_i = concentration of ith component, mol/kg_{HAc}
d_i = model parameters in eq 1
k_i = the rate constants, min^{-1}
r_i = rate of the ith step reaction, mol/(kg_{HAc}·min)

$[i]$ = mass concentration of substance i, kg/kg_{HAc}

Greek Letters

β and θ = kinetic parameters
ν_{ij} = stoichiometric coefficient of the jth component in the ith reaction

Subscripts

0 = initial conditions

Abbreviations

4-CBA = 4-carboxybenzaldehyde
$Co(Ac)_2$ = cobalt acetate
HAc = acetic acid
HBr = hydrogen bromide
$Mn(Ac)_2$ = manganese acetate
O_2 = oxygen
PT = *p*-toluic acid
PX = *p*-xylene
TA = terephthalic acid
TALD = *p*-tolualdehyde

Literature Cited

(1) Raghavendrachar, P.; Ramachadran, S. Liquid-Phase Catalytic Oxidation of *p*-Xylene. *Ind. Eng. Chem. Res.* **1992**, *31* (2), 453−462.

(2) Emanuel, N. M.; Gal, D. *Modelling of Oxidation Processes*; Akademiai Kiado: Budapest, Hungary, 1986.

(3) Cavalieri d'Oro, P.; Danoczy, E.; Roffia, P. On the Low Temperature Oxidation of *p*-Xylene. *Oxid. Commun.* **1980**, *1*, 153−155.

(4) Yan, X.; Du, W.; Qian, F. Development of a Kinetic Model for Industrial Oxidation of *p*-Xylene by RBF-PLS and CCA. *AIChE J*. **2004**, *50* (6), 1169−1176.

(5) Cao, G.; Pisu, M.; Morbidelli, M. A Lumped Kinetic Model for Liquid-phase Catalytic Oxidation of *p*-Xylene to Terephthalic Acid. *Chem. Eng. Sci.* **1994**, *49* (24), 5775−5788.

(6) Cao, G.; Servida, A.; Pisu, M. Kinetics of *p*-Xylene Liquid-phase Catalytic Oxidation. *AIChE J*. **1994**, *40* (7), 1156−1166.

(7) Cincotti, A.; Orrù, R.; Bori, A.; et al. Effect of Catalyst Concentration and Simulation of Precipitation Processes on Liquid-phase Catalytic Oxidation of *p*-Xylene to Terephthalic Acid. *Chem. Eng. Sci*. **1997**, *52* (21), 4205−4213.

(8) Cincotti, A.; Orrù, R.; Cao, G. Kinetics and Related Engineering Aspects of Catalytic Liquid-phase Oxidation of *p*-Xylene to Terephthalic Acid. *Catal. Today* **1999**, *52*, 331−347.

(9) Wang, L. Studies on the Kinetics of *p*-Xylene Oxidation and the Reactor Simulation. MS Thesis, Zhejiang University, China, 2001.

(10) Wang, Q.; Li, X.; Xie, G.; et al. Modeling of *p*-Xylene Oxidation Reactor-Condenser. *J. Zhejiang Univ.: Eng. Sci.* **2004**, *38* (8), 1029−1034.

(11) Cheng, Y.; Zhang, L.; Xie, G.; et al. Experiment Technique of *p*-Xylene Liquid-phase Oxidation. *Chem. React. Eng. Technol.* **2003**, *19* (2), 182−186.

(12) Digruov, N. G.; Dyakonov, J. A.; Lebedev, N. N.; et al. Kinetics of Liquid-Phase Oxidation of *p*-Xylene into Terephthalic Acid with a Cobalt Bromide Catalyst. *Izv. Vyssh. Uchebn. Zaved., Khim. Khim. Tekhnol.* **1970**, *13*, 407−412.

(13) Astarita, G.; Ocone, R. Chemical Reaction Engineering of Complex Mixtures. *Chem. Eng. Sci.* **1992**, *47* (9), 2135−2147.

Received for review July 18, 2004
Revised manuscript received October 24, 2004
Accepted November 9, 2004

IE049372X